Photophysical Investigations on Photoinitiators with Covalently Linked Thioxanthone Sensitizer Moieties

by **Kurt Dietliker** and **Stephanie Broillet**[1])

Ciba Specialty Chemicals Inc., Schwarzwaldallee 215, CH-4002 Basel

and

Bruno Hellrung, **Piotr Rzadek**, **Guenther Rist**, and **Jakob Wirz**

Department of Chemistry, University of Basel, Klingelbergstrasse 80, CH-4056 Basel

and

Dmytro Neshchadin and **Georg Gescheidt***

Institute of Physical and Theoretical Chemistry, Graz University of Technology, Technikerstrasse 4/I, A-8010 Graz

In memoriam Hanns Fischer

The photophysical properties of three photoinitiators with a covalently linked thioxanthone sensitizer unit absorbing up to 410 nm were investigated by laser-flash photolysis and CIDNP spectroscopy. These complementary techniques revealed two competing reaction pathways of the molecular dyads **1**–**3**: *i*) triplet-energy transfer from the sensitizer to the morpholine moiety followed by α-cleavage to yield a radical pair, which initiates radical polymerization, and *ii*) bimolecular electron transfer from the morpholine to the thioxanthone subunit followed by proton transfer. The relative efficiency of these routes is determined by the triplet energy of the photoinitiator moiety relative to that of the sensitizer.

1. Introduction. – Photoinitiators have been successfully utilized in the production of polymeric materials by radiation curing. Industrial applications of this technology providing considerable economic and ecological advantages are coatings, printing inks, electronic materials, as well as three-dimensional models and tools [1–3]. Although such initiators are rather efficient [4–12], it is possible to further enhance their activity by the addition of sensitizers [11][13]. This is especially useful when the sensitizer can be excited with light of different wavelengths than the photoinitiator, thereby adapting the action spectrum to specific requirements of the application. A typical case is the curing of pigmented formulations, where the excitation of the photoinitiator has to be performed in a transmission window of the pigment to allow sufficient penetration of light into the coating layer. While sensitization is usually achieved through diffusive encounters, we introduce here photoinitiators for radical polymeriza-

[1]) Current address: *UCB Farchim SA*, Z. I. de Planchy, 10, Chemin de Croix Blanche 1, CH-1630 Bulle.

tion in which a sensitizer (methyl 9-oxo-9*H*-thioxanthene-1-carboxylate) is covalently bound to the parent initiator molecule allowing intramolecular energy transfer.

Laser-flash photolysis (LFP) is an excellent tool to determine absolute reaction rates of excited states and short-lived intermediates. LFP does not, however, provide direct information regarding the chemical structure of the reactive intermediates involved in the reaction. Therefore, we have also applied CIDNP (chemically induced dynamic nuclear polarization). The spectral resolution provided by this NMR-based technique is appropriate to furnish molecular structures. Moreover, the polarizations of the NMR transitions indicate the multiplicity of the excited-state precursor and the pathway of product formation. Optical experiments can be performed at low concentrations ($< 10^{-4}$ M), conditions that favor monomolecular over bimolecular reactions. The concentrations required to provide satisfactory CIDNP signals are, however, larger by *ca.* two orders of magnitude than those used for LFP; concomitantly, intermolecular reactions become more likely.

We have chosen three candidates, **1**–**3**, in which the photoinitiator moieties are covalently linked to a thioxanthone sensitizer. How efficient are such bifunctional molecules? Is their reactivity a simple combination of the two functionalities or do additional (unexpected) reactions occur?

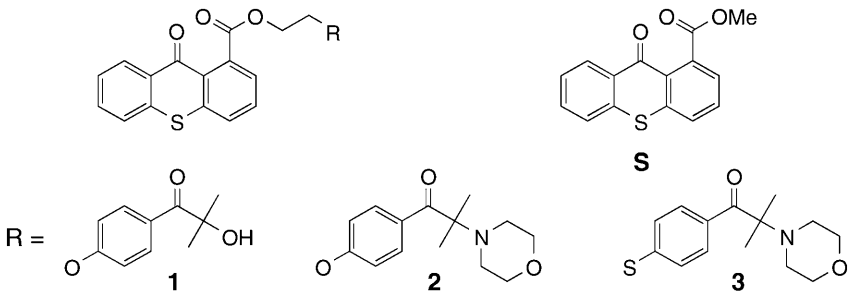

The three dyads represent three types of energy gaps between the triplet state of the sensitizer and that of the molecular moiety undergoing α-cleavage. In **1** [14], the triplet energy of the initiator moiety exceeds that of the sensitizer by *ca.* 8 kcal mol^{-1}, whereas in **2**, the triplet energies of the two components are similar. Finally in **3**, the situation is favorable for energy transfer to the initiator. These three models allow distinguishing between energy transfer and competing reactions. The parent thioxanthone **S** serves as a reference.

2. Experimental. – *LFP Measurements.* The LFP experiments were performed with degassed MeCN solns. (three freeze-pump-thaw cycles). A *Compex-205* excimer laser operating at 351 nm (XeF gas mixture, 100 mJ per pulse) was used for excitation. The absorbances of the solns. at 351 nm were chosen between 0.10 and 0.16 over the 1-cm excitation path length, corresponding to concentrations of the starting materials between 4.0 and $6.4 \cdot 10^{-5}$ M. Kinetic traces at selected wavelengths of observation were recorded with a *Tektronix-TDS-540* transient digitizer and analyzed by nonlinear least-squares fitting of the appropriate rate laws. A gated optical multichannel analyzer (time window 20 ns) was used to detect transient absorption spectra in the range between 250 and 750 nm and at preset time delays of between 25 ns and 100 μs with respect to the maximum of the laser pulse.

CIDNP. The CIDNP experiments were performed on a *Bruker AM-200* spectrometer equipped with a wide-bore magnet. A *Lambda-Physics* dye laser (diphenylstilbene soln.) pumped by a *Questek* excimer laser was used for excitation of perdeuterated MeCN solns. at λ 404.5 nm. At this wavelength, only the thioxanthone moiety shows significant absorption. The laser-pulse length was *ca.* 20 ns, the duration of the radiofrequency pulse 1–2 μs. The NMR absorptions were saturated immediately before the laser pulse. As a consequence, the spectra mainly exhibit polarized resonances of the photoproducts.

Calculations. Calculations were performed with the Gaussian03 package [15]. For geometry optimization and single-point determinations of the *Fermi* contacts (*i.e.*, isotropic hyperfine coupling constants, hfs), the UB3LYP/6-31G*//UHF/3-21G* protocol was used. This procedure generally provides rather accurate predictions of hfs [16][17].

Synthesis of Photoinitiators **1**–**3**. *9-Oxo-9*H-*thioxanthene-1-carboxylic Acid 2-[4-(2-Hydroxy-2-methyl-1-oxopropyl)phenoxy]ethyl Ester* (**1**). Potassium *tert*-butoxide (7.42 g, 0.02 mol) was added in portions to a soln. of 9*H*-9-oxothioxanthene-1-carboxylic acid (5.1 g, 0.02 mol) in DMSO (130 ml). The mixture was heated to 70°, and a soln. of methanesulfonic acid 2-[4-(2-hydroxy-2-methyl-1-oxopropyl)phenoxy]-ethyl ester [18] (7.42 g, 0.02 mol) was added dropwise with vigorous stirring. The temp. was kept at 70° for 90 min before the soln. was poured onto ice/water. The product was extracted with AcOEt, the soln. dried ($MgSO_4$), the solvent evaporated *in vacuo,* and the residual oil filtered over silica gel. The yellowish material was further purified by recrystallization from AcOEt/hexane: 5.82 g (55%) of **1**. M.p. 161–162° [19].

*9-Oxo-9*H-*thioxanthene-1-carboxylic Acid 2-{4-[2-Methyl-2-(morpholin-4-yl)-1-oxopropyl]phenoxy}ethyl Ester* (**2**). a) At r.t., 1-[4-(2-hydroxyethoxy)phenyl]-2-methyl-2-(morpholin-4-yl)-propan-1-one [20] (10.4 g, 0.035 mol) was treated with methanesulfonyl chloride (4.5 g, 0.038 mol) and Et_3N (3.95 g, 0.038 mol) in THF (25 ml). After stirring for 18 h, the mixture was poured on H_2O, the org. phase dried ($MgSO_4$), and the solvent evaporated: methanesulfonic acid 2-[4-(2-methyl-2-(morpholin-4-yl)-1-oxopropyl)phenoxy]ethyl ester. Yellowish oil that solidified upon standing and was used for the next reaction step without further purification.

b) Esterification of 9*H*-9-oxothioxanthene-1-carboxylic acid with the methanesulfonic acid ester from a) was performed as described for **1**: **2**. Yellowish solid. M.p. 122–128°.

*9-Oxo-9*H-*thioxanthene-1-carboxylic Acid 2-{{4-[2-Methyl-2-(morpholin-4-yl)-1-oxopropyl]phenyl}thio}ethyl Ester* (**3**). As described for **2**, except that methanesulfonic acid 2-{{4-[2-methyl-2-(morpholin-4-yl)-1-oxopropyl]phenyl}thio}ethyl ester was used. Yellowish solid. M.p. 135–139° [19][21].

3. Results and Discussion. – 3.1. *Structures of Initiators and Sensitizers.* Compounds **1**–**3** are composed of a thioxanthone sensitizer that is covalently bound to an acetophenone-type photoinitiator. Thioxanthone derivatives, in particular 2-isopropylthioxanthone (=2-isopropyl-9*H*-thioxanthen-9-one; **ITX**), find widespread use as sensitizers in radiation curing. Methyl 9-oxo-9*H*-thioxanthene-1-carboxylate (**S**) was chosen as the sensitizer component of dyads **1**–**3**, because it can be conveniently attached to a variety of hydroxy-substituted photoinitiators by esterification reactions and, importantly, possesses a triplet energy of 63 kcal mol^{-1} [22], which exceeds that of **ITX** (E_T = 61.4 kcal mol^{-1} [22]). In fact, compound **S** was found to be an efficient sensitizer for a variety of α-amino ketone type photoinitiators [22]. The initiator parts of the molecules **1**–**3** include the structural features of the very efficient α-hydroxy- and α-aminoacetophenone-type photoinitiators **P1**–**P3** [3][14][23]. Their triplet energies are summarized in the *Table.*

The 2-hydroxy-1-[4-(2-hydroxyethoxy)phenyl]-2-methylpropan-1-one (**P1**) is a commercial photoinitiator of the α-hydroxyacetophenone type, used for a variety of applications, mostly in nonpigmented formulations [24][25]. Transesterification of the thioxanthone derivative **S** with **P1** gives a straightforward access to compound **1**.

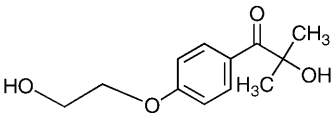

P1

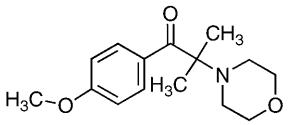

P2

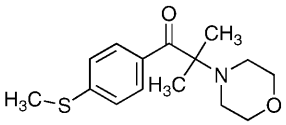

P3

Table. *Triplet Energies,* E_T, *of Photosensitizers* **ITX** *and* **S** *and Photoinitiators* **P1**–**P3**

	E_T/kcal·mol^{-1}	Ref.
ITX	61.4	[22]
S	63.0	[22]
P1	71.0	[14]
P2	65	[22]
P3	61	[22]

Compound **P2** is a representative of α-aminoacetophenone-type photoinitiators, which are used as very efficient photoinitiators for the curing of pigmented formulations. For the goal of this study, the MeO group in **P2** was transformed into a 2-hydroxyethoxy group that is suitable for covalent linking to the sensitizer **S**. The 2-methyl-1-[4-(methylthio)phenyl]-2-(morpholin-4-yl)propan-1-one (**P3**) is another commercial compound that has found widespread use as a very efficient photoinitiator in pigmented systems such as UV-curable printing inks and in resist formulations [26]. By analogy to **P2**, the *para*-(methylthio)-substituent in **P3** was transformed into a (2-hydroxyethyl)thio group to obtain a compound that can easily undergo reaction with the thioxanthone derivative **S**.

3.2. *Photochemical Reactions Determined by Optical Flash Photolysis.* 3.2.1. *General Considerations.* Before we discuss the results obtained with molecules **1**–**3**, we briefly describe the absorption spectra of the parent photoinitiators **P1**, **P2**, and **P3** (*Fig. 1*,*a*). Depending on the substitution pattern on the aromatic moiety, the absorption maxima are situated between 220 and 305 nm (solvent: MeCN) with only weak tailing into the region of 350–400 nm. The absorption of compounds **1**–**3** (*Fig. 1*,*b*) in that region is dominated by that of the thioxanthone chromophore with a maximum at 370 nm ($\varepsilon \approx 7 \cdot 10^3$ M^{-1} cm^{-1}). In practice, excitation of the photoinitiator with UV-A light is especially useful for the curing of blue-pigmented coatings that have a relatively high transmission at these wavelengths. Excitation by the lasers used (LFP: λ 351 nm; CIDNP: λ 404.5 nm), therefore, led to exclusive excitation of the sensitizer moiety.

3.2.1. *Thioxanthone* **S**. Intersystem crossing (ISC) of thioxanthone exhibits complex- and solvent-dependent kinetics, but population of the triplet state is predominantly fast (< 100 ps) and efficient [27]. Upon nanosecond LFP of **S**, very intense transient absorptions with maxima at 330 and 625 nm as well as bleaching of the ground-state absorption at 370 nm is generated during the laser flash (*Fig. 2*). The transient is assigned to the triplet state of **S**. The decay of triplet **S** obeys mixed-order kinetics due to a second-order contribution from triplet–triplet annihilation. The lifetime of the triplet of **S** was *ca.* 100 μs in degassed, dilute solutions. It was strongly reduced in the presence of triplet quenchers such as naphthalene or oxygen. Therefore, the life-

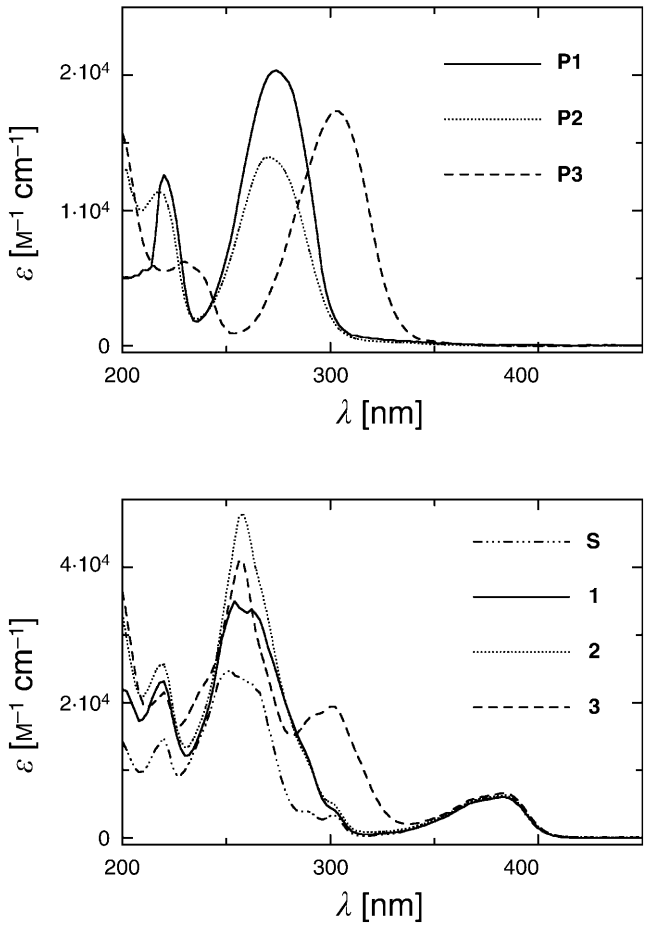

Fig. 1. *UV/VIS Absorption spectra of* a) **P1**–**P3** *and* b) **1**–**3**

time of the thioxanthone triplet state serves as a sensitive indicator for the rate of triplet-energy transfer to the initiator. LFP of **S** can be repeated several times without any detectable decrease of the signal intensities.

An estimate for the molar absorption coefficient ε of the triplet–triplet absorption at 625 nm may be derived from the initial amount of bleaching at 370 nm, $\Delta A \approx -0.3$. Because the initial absorbance at 625 nm is about twice as large, we may estimate the molar absorption coefficient of the triplet to be twice that of the ground state at 370, $\varepsilon_{TT,625} \approx 2 \cdot 10^4$ M^{-1} cm^{-1}.

3.2.2. *Initiator–Sensitizer Pair* **1**. Optical LFP of **1** in degassed MeCN was done at a concentration of $4 \cdot 10^{-5}$ M ($A_{351} = 0.1$). The results resemble those obtained with parent **S** (see insert, *Fig. 2*). In particular, the half-life of the sensitizer triplet is not affected showing that energy transfer from the sensitizer to the initiator does not occur. This is not unexpected, because the triplet energy of **P1** of 71 kcal mol^{-1} is considerably higher than that of **S** (63 kcal mol^{-1}, *Table*).

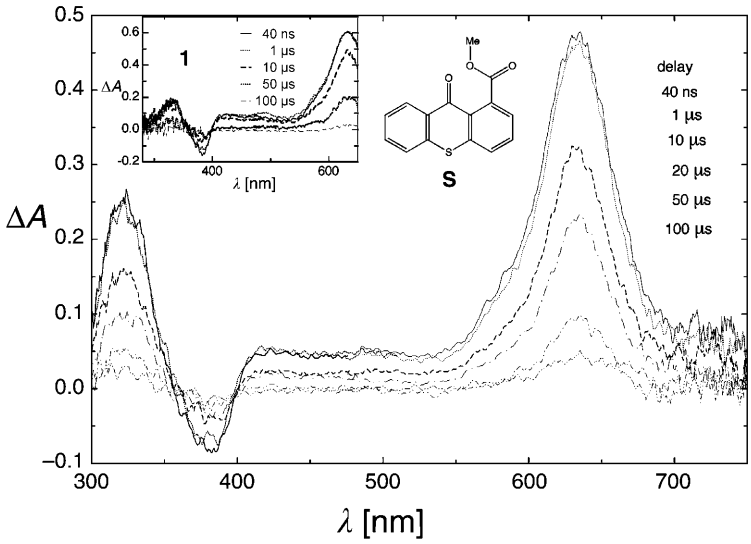

Fig. 2. *Transient spectra obtained by LFP of* **S**. The insert shows analogous spectra of **1**.

3.2.3. *Initiator–Sensitizer Pair* **2**. With triplet energies of 63 (**S**) and 65 kcal mol^{-1} (**P2**) (*Table*), the dyad **2** represents a borderline case for energy transfer. Here, the decay of the triplet absorption obeys a first-order law accurately with a lifetime of τ 1.4 µs. With the decay of the triplet, a new, very broad transient with a maximum at 520 nm is built up, which subsequently disappears within 40 µs (*Fig. 3*). Excitation of **2** is largely irreversible: a single laser flash led to *ca.* 50% decomposition.

LFP of the sensitizer **S** in the presence of initiator **P2** also led to a reduction of the triplet lifetime of **S**, but no 520-nm transient was detected. The seventy-fold reduction of the triplet lifetime of **2** relative to that of **S** is attributed to intramolecular triplet-energy transfer. We tentatively assign the 520-nm transient to a triplet charge-transfer state of **2**. Here, the CIDNP experiments provide additional insight (*vide infra*).

3.2.4. *Sensitizer–Initiator Pair* **3**. As the initiator **P3** has a triplet energy of 61 kcal mol^{-1} (*Table*), *i.e.*, lower than that of thioxanthone, dyad **3** is the best candidate for intramolecular sensitization. Indeed, LFP experiments with **3** clearly show that triplet-energy transfer from the thioxanthone fragment is very fast and efficient. Concentrations of the starting material were $5 \cdot 10^{-5}$ M, $A_{351} = 0.15$. The laser-pulse energies were *ca.* 100 mJ. The strong triplet transient, λ_{max} 625 nm, decayed much faster than that of **2**, $k \approx 2 \cdot 10^7\ s^{-1}$. No other transient absorptions were observed after the first flash. Further flashes produced transients arising from the excitation of photoproducts (see discussion of CIDNP experiment). As in the case of **2**, the photoreactions of **3** are irreversible, and **3** was largely decomposed by a single photoflash.

The fast decay observed for the sensitizer triplet of **3** is again attributed to energy transfer. Triplet-energy transfer requires contact between the donor and acceptor moieties, and the observed rate constant for this process, $k \approx (5-6) \cdot 10^7\ s^{-1}$, is indeed of the order of magnitude expected for the contact rate between sensitizer and initiator through conformational changes of the saturated linker [28].

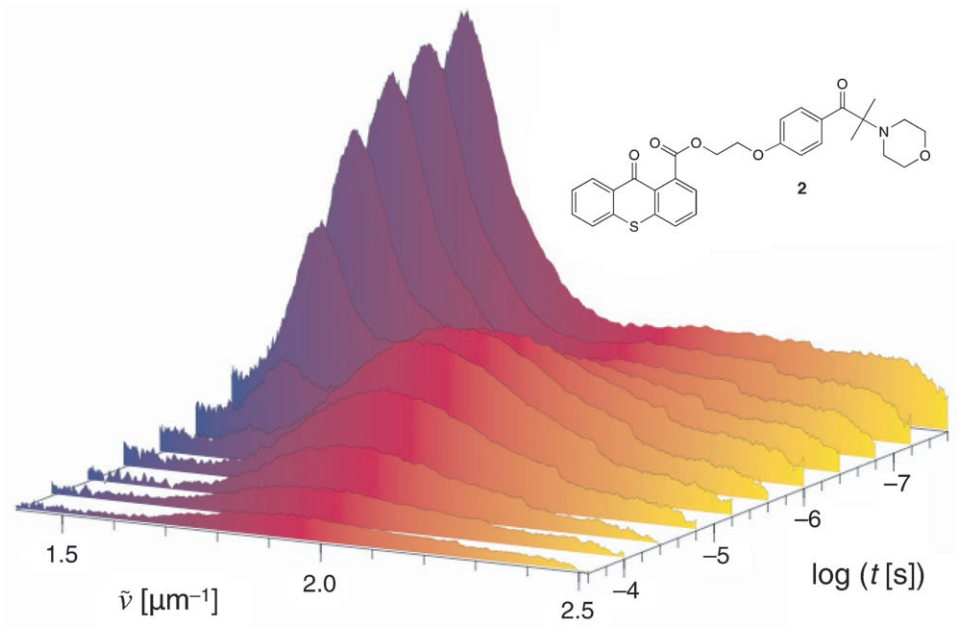

Fig. 3. *3-D Plot of transient absorption spectra at various delays after the laser pulse obtained by LFP of* **2** *in degassed MeCN*

3.3. *Photochemistry as Deduced by CIDNP.* 3.3.1. *General Considerations.* Whereas the optical measurements provided mainly kinetic information, CIDNP provides insight into the photophysical reaction pathways and the structure of the photoproducts. Because application of the CIDNP technique affords higher concentrations (*ca.* 10^{-4} M) of the reactants, it was necessary to consider also bimolecular reactions: With a diffusion coefficient reasonable in liquid solutions of *ca.* 10^{10} s^{-1} mol^{-1} l and a concentration of 10^{-4} mol l^{-1}, the rate of molecular encounter can be estimated as *ca.* 10^{6} s^{-1}. This rate is at least one order of magnitude slower than that determined for intermolecular energy transfer in **2** and **3**. Accordingly, intermolecular energy transfer should not play a major role when CIDNP effects are observed. This is moreover illustrated by kinetic simulations represented in the *Supplementary Material*[2]).

On the other hand, for electron-transfer reactions, nuclear-polarization patterns indicate that bimolecular processes play an important part (particularly for **2**, see below). Internal biradical reactions can hardly be detected by CIDNP in the present case.

3.3.2. *Previous Results.* In an earlier investigation, CIDNP experiments were performed with mixtures of **S** and **P1**–**P3** [22]. It was established that the triplet state of **S** can be transferred to an initiator with lower triplet energy in apolar and to a smaller extent in polar solvents. The sensitization was much more efficient for **P3** than for **P2**. Initiator **P1** could not be sensitized with **S**, as expected from the corresponding triplet energies. The primary radicals of initiators **P2** and **P3** were converted to (substituted)

[2]) *Supplementary Material* can be obtained from the authors.

benzaldehydes and an enamine. Besides energy transfer, the polarizations pointed to initial electron-transfer reactions followed by H^+-transfer in the primary cage, as experienced for photoinitiators containing amino groups. Fast reactions of 2-(morpholin-4-yl)propyl radicals with oxygen lead to acetone and a hypothetical morpholin-4-yl radical, which in the case of initiator **P3** finally leads to 4-(4-(methylthio)benzoyl)morpholine. This product was identified by preparative irradiation experiments and by NMR spectroscopy. Escape reactions led to the formation of products stemming from either two substituted benzoyl or two substituted methyl radicals.

3.3.3. *CIDNP of* **1**. As expected and in analogy to the observations from the LFP measurements, no photoproducts were detected after photolysis of **1** inside the NMR probehead.

3.3.4. *CIDNP of* **2**. In *Fig. 4*,*a*, the CIDNP spectrum of **2**, obtained after several laser flashes at 404.5 nm, is reproduced. The signals are assigned in the following way: The weak resonance at δ 9.98 (*vs.* $SiMe_4$) is assigned to aldehyde **7** (*Scheme 2*) and reveals α-cleavage after triplet transfer. The resonances attributable to an enamine, formed in the primary pair reaction, are very weak and broadened in the presence of oxygen (not visible in *Fig. 4*,*a* but detected in [14], see *Scheme 2*). The dominant polarized resonance (enhanced absorption) in *Fig. 4*,*a* is a *d* at δ 5.83, accompanied by a weakly enhanced one at δ 5.33. These signals are assigned to the olefinic protons H–C(3) and H–C(2) of structure **9** (*Scheme 3*; analogous to **5** in *Scheme 1*, formed from **S** and **4**, *vide infra*). These two chemical shifts as well as the coupling constant between the two protons of *ca.* 5.5 Hz are in good agreement with literature values of didehydrogenated morpholine moieties. [29]. Moreover, in the NMR product analysis, double-resonance experiments established the connection between the two protons of the C=C bond in the oxidized morpholine moiety.

Such a product is likely to be formed *via* electron transfer as described previously [22]. After initial electron transfer between the **S** and the morpholine moieties of **2**, a proton of the CH_2(2) group (or, analogously of the CH_2(6) group) and, subsequently, adjacent H-atoms can be transferred from the morpholinyl substituents either to the primary radicals or to a triplet-excited **S** with the formation of the partly dehydrogenated morpholinyl derivative **9** (*Scheme 3*). Polarization may be built up in the primary radical-ion pair or in the final radical pair after proton-transfer (or, alternatively, H-atom transfer, if H-abstraction takes place). Indeed, polarization of the signals attributed to the NCH_2 groups of the starting material reveal the electron-transfer pathway [22] (note that experiments in this work and [22] were performed in different solvents). Additional mechanistic insights follow from the analysis of the polarization intensities. The strongly enhanced absorption at δ 5.83 points to a strong positive isotropic proton hyperfine coupling, ^{1}H-hfs, of the OCH_2 moiety in the final radical pair. The weak signal intensity at δ 5.33 represents an overlay of polarization processes in the ionic *and* in the final radical pair. This requires ^{1}H-hfs with different signs for the protons in 2-positions of the morpholine moiety in radical-ion pair $\mathbf{2}^{\bullet-}/\mathbf{2}^{\bullet+}$ and the final radical pair **2a**$^\bullet$/**2b**$^\bullet$ (see *Scheme 3*). This is corroborated by model calculations (B3LYP//6-31G*) of $\mathbf{P2}^{\bullet+}$ and $\mathbf{4}^\bullet$ (*Fig. 5* representing analogs of the precursors of the dehydrogenated morpholine moiety in **9**).

The ^{1}H-hfs of the CH_2(3) protons are positive for both radicals, giving rise to the enhanced absorption at δ 5.83 in line with *Kaptein*'s rules assuming a higher *g* value

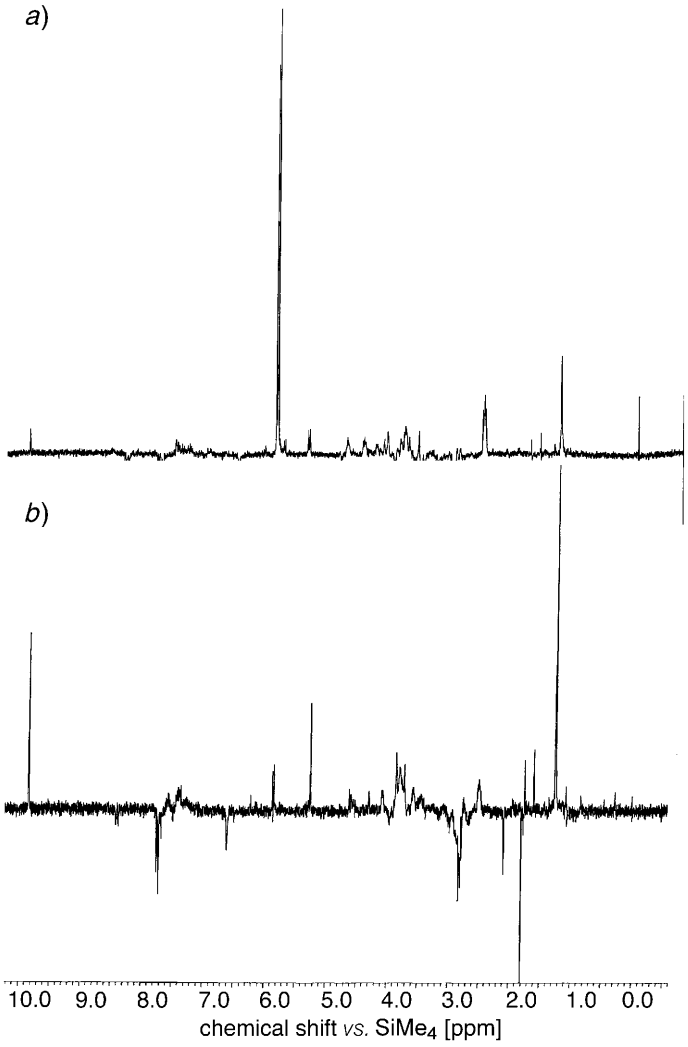

Fig. 4. *^{1}H-CIDNP Spectra of* a) **2** *and* b) **3**. For exper. conditions, see *Sect. 2, Exper.*

for the N-containing radicals than in the **S**-derived ones (*Fig. 6*). On the other hand, the ^{1}H-hfs of H–C(2) in $\mathbf{P2}^{\bullet+}$ is positive (+3.99 mT) but carries a negative sign in $\mathbf{4}^{\bullet}$ (−1.42 mT, *Fig. 5*). Accordingly, the intensity of the resonance attributed to H–C(2) in product **9** is expected to be considerably lower; this is perfectly reflected by the experiment (*Fig. 4,a*).

Moreover, the pronounced enhanced absorption of the NCH_2 group at δ 2.52 of parent **2** (*Fig. 4,a*) shows that back electron transfer to the parent thioxanthone moiety takes place. This is also supported by the emissive polarizations of the **S** part between δ 7.5 and 8.6 (based on the intermediate radical anion $\mathbf{S}^{\bullet-}$ and $\mathbf{SH}^{\bullet}$), which are pronounced for the positions of the highest calculated ^{1}H-hfs (*Fig. 6*), which are all nega-

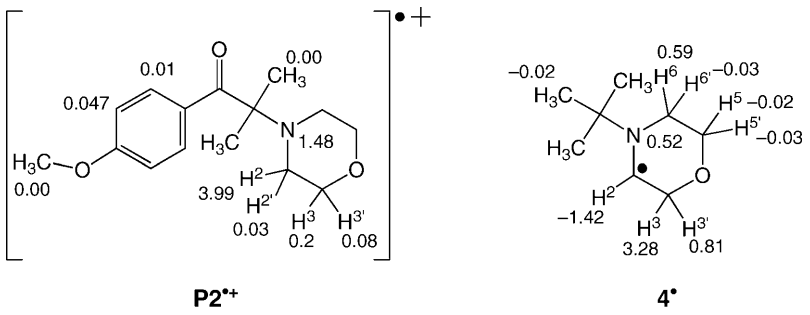

P2$^{\bullet+}$ **4**$^{\bullet}$

Fig. 5. *Calculated* (UB3LYP//6-3G*) ^{1}*H-hfs* [mT] *of* **P2**$^{\bullet+}$ *and* **4**$^{\bullet}$

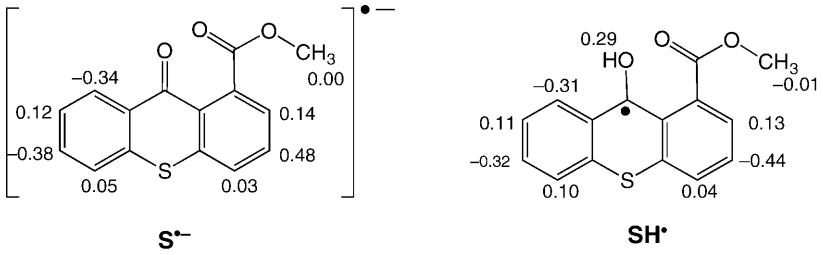

S$^{\bullet-}$ **SH**$^{\bullet}$

Fig. 6. *Calculated* (UB3LYP//6-3G*) ^{1}*H-hfs* [mT] *of* **S**$^{\bullet-}$ *and* **SH**$^{\bullet}$

tive. The polarizations are again compatible with *g* values larger for the morpholine than for the thioxanthone radicals.

An emission at δ 6.36 is tentatively assigned to the C(OH)*H* ring proton of the hydrogenated thioxanthone in **10** (see *Scheme 3*). The literature value for a related molecule is δ 5.57 ($CDCl_3$), and calculations suggest a δ value of 5.57 ± 0.07. Assuming a cage reaction, however, the polarization (emission) cannot be explained in a straightforward way. Probably, this derivative is formed in a number of ways, as cage and escape product in the photoinduced electron-transfer pathways, or in a reaction between the substituted aldehyde and the **S**$^{\bullet}$ moiety. A possibility for an escape product would be disproportionation between two **SH**$^{\bullet}$ radicals as illustrated in *Scheme 1* for the model reaction.

3.3.5. *CIDNP of* **3**. The relatively strong resonance (enhanced absorption) of aldehyde **8** at δ 9.98 (*Fig 4*, *b*) again confirms α-cleavage in the excited triplet state for this initiator. The resonance of enamine **11** at δ 5.83 is again detected, however, with a relatively low intensity indicating that photoinduced electron transfer (*Scheme 3*) is much less pronounced in the case of **3** than for **2**. An emission-type resonance at approximately δ 2.10 is tentatively assigned to acetone (**6**), formed by oxidation of the substituted alkyl radical in the primary α-cleavage pair (*Scheme 2*).

Initiator **3** exhibits strong α-cleavage and, in contrast to **2**, much less pronounced electron transfer (mainly detected *via* the oxidized morpholine moiety transient at δ 5.83 (**11**) and the polarization of the starting material at δ 2.52). In agreement with the favorable triplet energies of the components **S** and **P3,** triplet transfer is much more efficient for **3** than for **2**.

3.3.6. *CIDNP of* **S** *and 4-(*tert*-Butyl)morpholine* (**4**). To verify the electron transfer between the **S** and morpholine moieties of **2** and **3**, a CIDNP experiment was performed with a mixture of **S** and 4-(*tert*-butyl)morpholine (**4**; *Fig. 7*). Again the characteristic resonance at δ 5.83 is detected representing the formation of the C=C bond in the dehydrogenated compound **5** (*Scheme 1*).

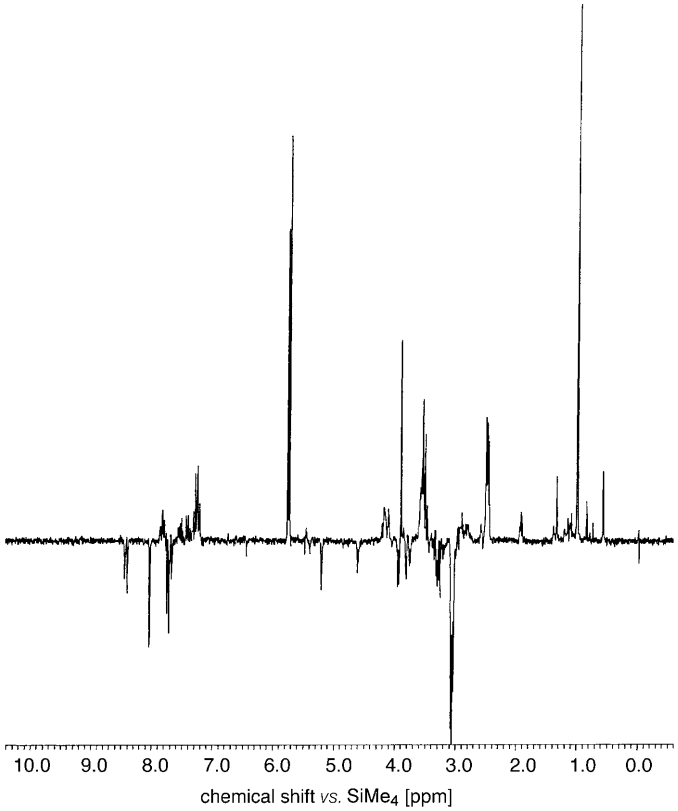

Fig. 7. *^{1}H-CIDNP Spectrum for the intermolecular energy/electron transfer between* **S** *and* **4**. For exper. conditions, see *Sect. 2, Exper.*

4. Fusion of LFP and CIDNP. – Two principal photochemical channels for the decay of **2** and **3** were established by the optical experiments and CIDNP: *i*) Energy transfer followed by α-cleavage (*Scheme 2*), and *ii*) formation of an intermolecular and/or intramolecular charge-transfer complex with subsequent electron and H^+/H transfer (*Scheme 3*). The balance between these two pathways is determined by the relative rate constants of energy and electron transfer for **2** and **3**.

The rate constants assigned to energy transfer in **2** and **3** are *ca.* $7 \cdot 10^5$ s^{-1} and $2 \cdot 10^7$ s^{-1}, respectively. Why is energy transfer *ca.* 30 times slower in the case of **2**? As the linker chain is the same in molecules **2** and **3**, we conclude that the encounter rate is not decisive for the rate of energy transfer in **2**. Essentially, small structural differences between the ground- and triplet-state structures of donor and acceptor cause an addi-

Scheme 1. *Irradiation of Sensitizer* **S** *in the Presence of* N-*(*tert-*Butyl)morpholine* (**4**). The polarized signal attributed with $\mathbf{SH_2}$ can not be unambiguously distinguished in *Fig. 7.*

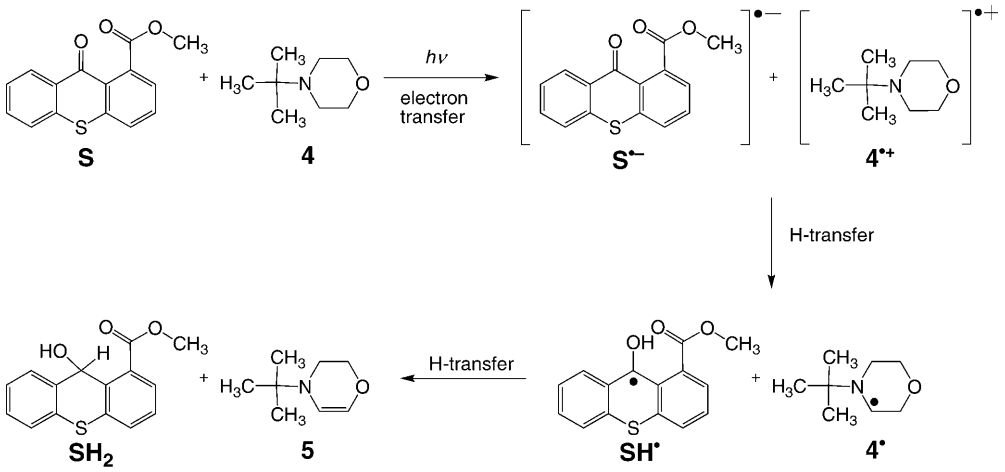

Scheme 2. *Products After Intramolecular Energy Transfer in* **2** *and* **3** *Established by LFP and CIDNP*

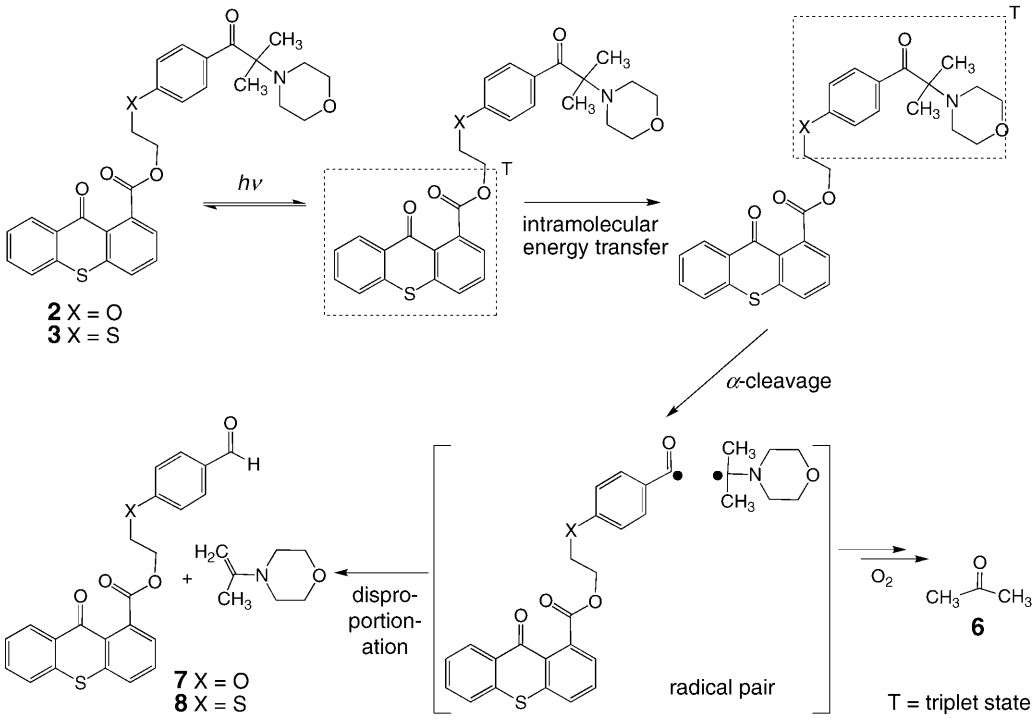

tional small energy barrier ('nonvertical energy transfer' [30]). With **2** and **3** possessing rather similar geometries, the significantly slower rate of energy transfer in **2** can be predominately traced back to the slightly endothermic character of energy transfer

Scheme 3. *Products After Intra- or Intermolecular Electron Transfer* (for LFP, only the formation of the charge-transfer state **9** or the radical ion pair $\mathbf{2}^{\bullet-}/\mathbf{2}^{\bullet+}$ is established, whereas CIDNP polarizations reveal the presence of $\mathbf{2}^{\bullet-}/\mathbf{2}^{\bullet+}$ and their follow-up products)

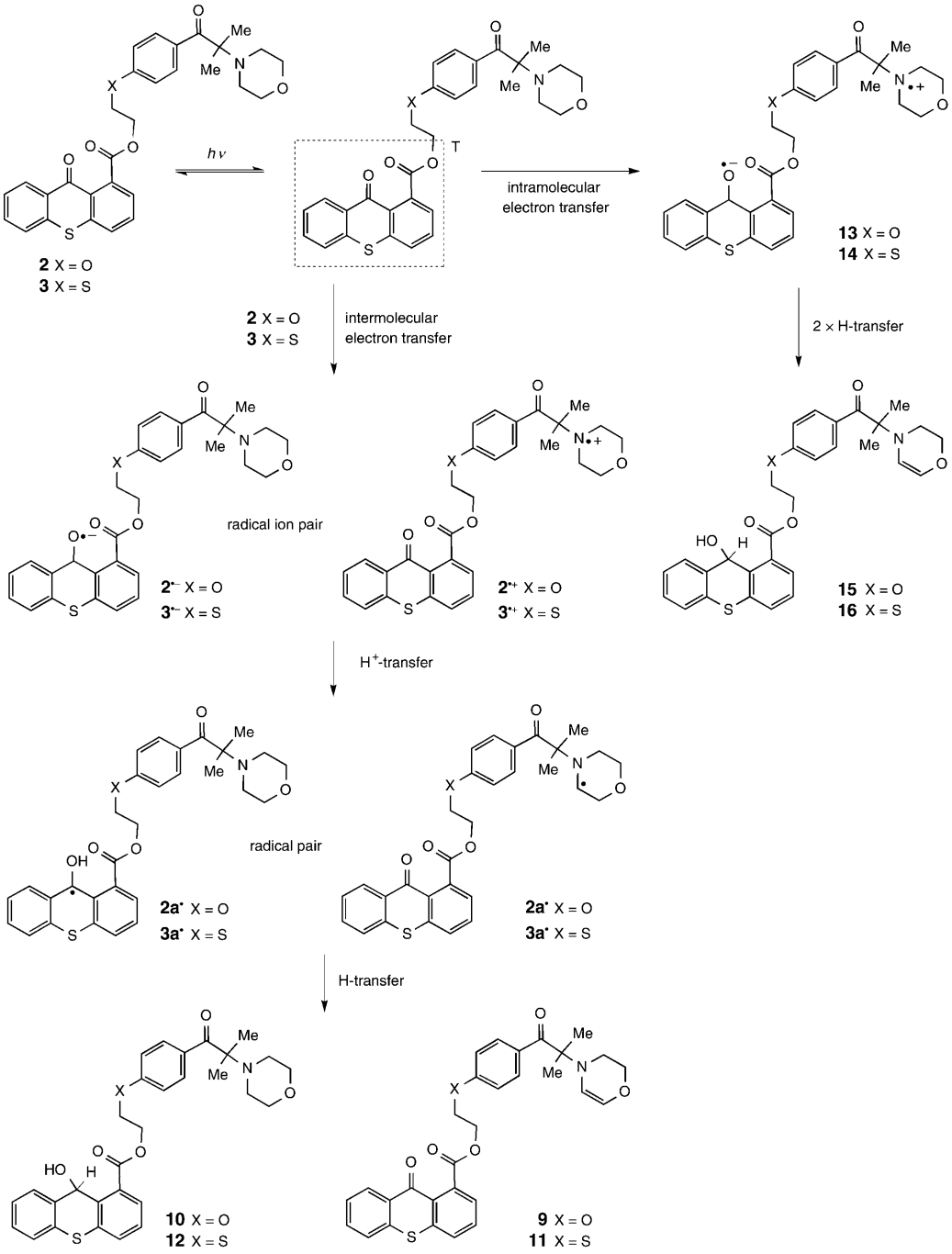

(*Table*). Using the *Sandros* equation [31] to estimate the difference for the rate of triplet transfer in **2** and **3**, a factor of 29 (*T* 298 K) is calculated. This value virtually matches the experimental one.

The first-order rate constants of intramolecular energy transfer have to be compared with the rate of intermolecular electron transfer. For **S** and 4-(*tert*-butyl)morpholine (**4**), a paradigm for the morpholine moiety (acting as the electron donor) in **2** and **3**, a bimolecular rate constant, k_{ET}, of *ca.* 10^8 M^{-1} s^{-1} ($3.6 \cdot 10^8$ M^{-1} s^{-1} in toluene and $8.3 \cdot 10^8$ M^{-1} s^{-1} in MeOH) was determined [22]. Accordingly, in the case of **2**, intermolecular electron transfer becomes a well detectable reaction pathway (in the concentration range of the LFP and CIDNP experiment), being *ca.* two orders of magnitude faster than energy transfer. On the other hand, for **3**, observation of the intermolecular reaction is not conceivable for 10^{-5} M concentrations (LFP) and only marginally detectable at the higher concentrations in the CIDNP experiments.

Generally, only the products formed *via* the radical ion pairs $\mathbf{2}^{\bullet-}/\mathbf{2}^{\bullet+}$ and $\mathbf{3}^{\bullet-}/\mathbf{3}^{\bullet+}$, *i.e.* **9**–**12** can be established by CIDNP. The presence of charge-transfer state **13** could be connected to the broad absorption at 520 nm, the analogous stage for **3**, charge-transfer state **14** is not detectable as are tentative products **15** and **16** (*Scheme 3*).

5. Conclusions. – We demonstrated that intramolecular sensitization is feasible for photoinitiators **2** and **3**. To establish the photochemical reactions of the excited initiator fragment after the triplet transfer, laser-flash photolysis and CIDNP experiments were performed. The products were identified and compared with the reactions of initiator–sensitizer mixtures. In the CIDNP experiments, additional bimolecular electron-transfer reactions were detected, particularly in the case of **2**.

Bimolecular energy transfer from the sensitizer **S** to the initiator **P2** was not detected in benzene and was only weakly perceivable in MeOH [22]. For dyad **2** which joins these components through a covalent bridge, it was readily observed in MeCN solution. The intramolecular triplet transfer is considerably slower for **2** than for **3**. Consequently, energy transfer in **2** competes with electron-transfer and subsequent proton-transfer reactions.

Generally, photoinitiator–sensitizer dyads can be regarded as ideal candidates for the initiation of radical-based reactions, when only very low amounts of initiator can be used and irradiation has to be performed at wavelengths that are red-shifted with respect to the absorption spectrum of the initiator. Obviously, the triplet energy of the sensitizer moiety has to be higher than that of the photoinitiator although the energy-transfer efficiency in the borderline case of **2** is remarkable. Moreover, the two reaction channels, α-cleavage and electron transfer, established for **2**, suggest that such molecules could be utilized as mechanistic tools in reactions with competitive pathways.

REFERENCES

[1] K. Dietliker, T. J. Jung, J. Benkhoff, H. Kura, A. Matsumoto, H. Oka, D. Hristova, G. Gescheidt, G. Rist, *Macromol. Symp.* **2004**, *217*, 77.

[2] P. Chabrecek, K. Dietliker, D. Lohmann, to *Ciba-Geigy AG*, PCT Int. Appl. WO 9620919 A1 (priority date 30.12.1994).

[3] V. Desobry, K. Dietliker, R. Huesler, W. Rutsch, M. Rembold, F. Sitek, to *Ciba-Geigy AG*, Eur. Pat. Appl. EP 284561 A2 (priority date 26.3.1987).
[4] I. Gatlik, P. Rzadek, G. Gescheidt, G. Rist, B. Hellrung, J. Wirz, K. Dietliker, G. Hug, M. Kunz, J.-P. Wolf, *J. Am. Chem. Soc.* **1999**, *121*, 8332.
[5] D. Hristova, I. Gatlik, G. Rist, K. Dietliker, J.-P. Wolf, J.-L. Birbaum, A. Savitsky, K. Möbius, G. Gescheidt, *Macromolecules* **2005**, *38*, 7714.
[6] C. S. Colley, D. C. Grills, N. A. Besley, S. Jockusch, P. Matousek, A. W. Parker, M. Towrie, N. J. Turro, P. M. W. Gill, M. W. George, *J. Am. Chem. Soc.* **2002**, *124*, 14952.
[7] S. Jockusch, N. J. Turro, *J. Am. Chem. Soc.* **1998**, *120*, 11773.
[8] G. W. Sluggett, C. Turro, M. W. George, I. V. Koptyug, N. J. Turro, *J. Am. Chem. Soc.* **1995**, *117*, 5148.
[9] M. Weber, I. V. Khudyakov, N. J. Turro, *J. Phys. Chem., A* **2002**, *106*, 1938.
[10] M. Weber, N. J. Turro, *J. Phys. Chem., A* **2003**, *107*, 3326.
[11] R. M. Williams, I. V. Khudyakov, M. B. Purvis, B. J. Overton, N. J. Turro, *J. Phys. Chem., B* **2000**, *104*, 10437.
[12] G. W. Sluggett, P. F. McGarry, I. V. Koptyug, N. J. Turro, *J. Am. Chem. Soc.* **1996**, *118*, 7367.
[13] R. Liska, *J. Polymer Sci., A* **2004**, *42*, 2285.
[14] S. Jockusch, M. S. Landis, B. Freiermuth, N. J. Turro, *Macromolecules* **2001**, *34*, 1619.
[15] M. J. Frisch, G. W. Trucks, H. B. Schlegel, G. E. Scuseria, M. A. Robb, J. R. Cheeseman, J. A. Montgomery, T. Vreven, K. N. Kudin, J. C. Burant, J. M. Millam, S. S. Iyengar, J. Tomasi, V. Barone, B. Mennucci, M. Cossi, G. Scalmani, N. Rega, G. A. Petersson, H. Nakatsuji, M. Hada, M. Ehara, K. Toyota, R. Fukuda, J. Hasegawa, M. Ishida, T. Nakajima, Y. Honda, O. Kitao, H. Nakai, M. Klene, X. Li, J. E. Knox, H. P. Hratchian, J. B. Cross, V. Bakken, C. Adamo, J. Jaramillo, R. Gomperts, R. E. Stratmann, O. Yazyev, A. J. Austin, R. Cammi, C. Pomelli, J. W. Ochterski, P. Y. Ayala, K. Morokuma, G. A. Voth, P. Salvador, J. J. Dannenberg, V. G. Zakrzewski, S. Dapprich, A. D. Daniels, M. C. Strain, O. Farkas, D. K. Malick, A. D. Rabuck, K. Raghavachari, J. B. Foresman, J. V. Ortiz, Q. Cui, A. G. Baboul, S. Clifford, J. Cioslowski, B. B. Stefanov, G. Liu, A. Liashenko, P. Piskorz, I. Komaromi, R. L. Martin, D. J. Fox, T. Keith, M. A. Al-Laham, C. Y. Peng, A. Nanayakkara, M. Challacombe, P. M. W. Gill, B. Johnson, W. Chen, M. W. Wong, C. Gonzalez, J. A. Pople, 'Gaussian 03, Revision C.02', *Gaussian Inc*., Wallingford CT, 2004.
[16] R. Batra, B. Giese, M. Spichty, G. Gescheidt, K. N. Houk, *J. Phys. Chem.* **1996**, *100*, 18371.
[17] L. Hermosilla, P. Calle, J. M. G. de la Vega, C. Sieiro, *J. Phys. Chem., A* **2005**, *109*, 1114.
[18] B. Müller, to *Ciba-Geigy AG*, PCT Int. Appl. WO 9624077 A1 (priority date: 3.2.1995).
[19] M. Koehler, J. Ohngemach, to *Merck GmbH*, Eur. Pat. Appl. 354458 A2 (priority date: 9.8.1988).
[20] P. Chabrecek, D. Lohmann, K. Dietliker, to *Ciba-Geigy AG*, PCT Int. Appl. WO 9621167 A1 (priority date 30.12.1994).
[21] H. Yamato, M. Ohwa, T. Asakura, A. Matsumoto, to *Ciba Speciality Chemicals Holding Inc.*, PCT Int. Appl. WO 2000068218 A1 (priority date: 10.5.1999).
[22] G. Rist, A. Borer, K. Dietliker, V. Desobry, J. P. Fouassier, D. Ruhlmann, *Macromolecules* **1992**, *25*, 4182.
[23] D. Leopold, H. Fischer, *J. Chem. Soc., Perkin Trans. 2* **1992**, 513.
[24] A. F. Cunningham, V. Desobry, K. Dietliker, R. Huesler, D. G. Leppard, *Chimia* **1994**, *48*, 423.
[25] K. Vacek, J. Geimer, D. Beckert, R. Mehnert, *J. Chem. Soc., Perkin Trans. 2* **1999**, 2469.
[26] B. F. Howell, A. de Raaff, T. Marino, *ACS Symp. Ser.* **1997**, *673*, 219.
[27] C. Ley, F. Morlet-Savary, P. Jacques, J. P. Fouassier, *Chem. Phys.* **2000**, *255*, 335.
[28] O. Bieri, J. Wirz, B. Hellrung, M. Schutkowski, M. Drewello, T. Kiefhaber, *Proc. Natl. Acad. Sci. U.S.A.* **1999**, *96*, 9597.
[29] F. P. Colonna, G. Distetano, S. Pignataro, G. Pittaco, E. Valentin, *J. Chem. Soc., Faraday Trans. 2* **1975**, *71*, 1572.
[30] V. Balzani, F. Bolletta, F. Scandola, *J. Am. Chem. Soc.* **1980**, *102*, 2152.
[31] K. Sandros, *Acta Chem. Scand.* **1964**, *8*, 2355.

Received April 06, 2006